Droop-free Team-oriented Control for AC Distribution Systems

Nasirian, Vahidreza ; Shafiee, Qobad; Guerrero, Josep M.; Lewis, Frank; Davoudi, Ali

Published in:
Proceedings of the 2015 IEEE Applied Power Electronics Conference and Exposition (APEC)

DOI (link to publication from Publisher):
10.1109/APEC.2015.7104764

Publication date:
2015

Document Version
Early version, also known as pre-print

Droop-free Team-oriented Control for AC Distribution Systems

Vahidreza Nasirian, Qobad Shafiee, Josep M. Guerrero, Frank L. Lewis, and Ali Davoudi

***Abstract*— Droop control is conventionally used for load sharing in AC distribution systems. Despite decentralized nature of the droop technique, it requires centralized secondary control to provide voltage and frequency regulation across the system. Distributed control, as an alternative to the centralized controller, offers improved reliability and scalability. Accordingly, a droop-free distributed framework is proposed that fine-tunes the voltage and frequency at each source to handle 1) Voltage regulation, 2) Reactive power sharing, 3) Frequency synchronization, and 4) Active power sharing. The controller includes three modules, namely, voltage regulator, reactive power regulator, and active power regulator. The voltage regulator boosts the voltage across the distribution system to satisfy the global voltage regulation. Proportional load sharing is adopted, where the total load is shared among sources in proportion to their rated powers. The active power regulator addresses frequency synchronization without using any frequency feedback/measurement, which improves the system dynamic. Simulation results are provided to verify the performance of the proposed control methodology.**

***Index Terms*— AC microgrids, Cooperative control, Distributed control, Droop control, Inverter.**

I. Introduction

Microgrids are small-scale power systems that have gained popularity in distribution systems for their improved efficiency, reliability, and expandability [1], [2]. Inverters are commonly used to integrate energy resources, e.g., photovoltaic arrays, storage elements, and fuel cells, to the AC microgrid distribution network [3]. A three-tier hierarchical control structure is conventionally adopted for the microgrid operation [4]. The primary control, usually implemented by a droop mechanism, operates on a fast timescale and regulates inverters' output voltage and handles load sharing among inverters [5].

This work was supported in part by the National Science Foundation under grants ECCS-1137354 and ECCS-1405173 and in part by the U.S. Office of Naval Research under grant N00014-14-1-0718. Vahidreza Nasirian, Frank L. Lewis, and Ali Davoudi are with the Department of Electrical Engineering, University of Texas, Arlington, TX 76019 USA and are also with the University of Texas at Arlington Research Institute (UTARI), Fort Worth, TX 76118 USA (emails: vahidreza.nasirian@mavs.uta.edu; lewis@uta.edu; davoudi@uta.edu). Qobad Shafiee and Josep M. Guerrero are with the Department of Energy Technology, Aalborg University, Denmark. Qobad Shafiee was also on leave with the University of Texas, Arlington, TX. (Emails: qsh@et.aau.dk; joz@et.aau.dk).

The secondary control compensates for the voltage and frequency deviations caused by the primary control by updating the voltage and frequency set points [6], [7]. Ultimately, the tertiary control carries out the scheduled power exchange between the microgrid and the main grid [8].

Droop mechanism is a common decentralized approach to realize the primary control. It emulates virtual inertia for AC systems and mimics the role of governors in traditional synchronous generators [9]. Despite simplicity, the droop mechanisms suffers from 1) load-dependent frequency/voltage deviation, 2) poor transient performance for nonlinear loads [10], and 3) poor reactive power sharing in presence of unequal bus voltages. Unequal bus voltages are essential to perform the scheduled reactive power flow. Droop techniques cause voltage and frequency deviations. Thus, the supervisory secondary control updates the set points of the local primary control [11]–[13]. Such central controllers require two-way high-bandwidth communication links between the controller and each inverter. This design compromises the system reliability as failure of any communication link hinders the overall controller functionality. The central controller is also a single-point of failure that introduces another reliability risk. Scalability is another issue because it adds to the complexity of the communication network.

Spatially dispersed inverter-based microgrids naturally lend themselves to distributed control techniques to address the synchronization and coordination requirements. Distributed control architectures can discharge duties of a central controller while being resilient to faults or system uncertainties. Distributed control processes necessitate that each agent (i.e., the inverter) exchange information with other agents according to some restricted communication protocol [14], [15]. These controllers use a sparse communication network and have less computational complexity at each inverter controller [16]. Networked control of parallel inverters in [17] embeds the functionality of the secondary control in all inverters and requires a fully connected communication network. The master node in the networked master-slave methods [18]–[20] is still a single point-of-failure. Distributed cooperative control is recently introduced for DC and AC microgrids [21]–[27]. Distributed control of AC microgrids are discussed in [28], [29]. The majority of such approaches are still based on the droop control (and, thus, inherit its shortcoming), require system information (e.g.,

number of inverters, inverter parameters, total load demand), and mainly handle active power sharing and frequency regulation (or only reactive power sharing/voltage regulation).

This paper provides a droop-free distributed cooperative solution that satisfies the secondary/primary control objectives for an autonomous AC microgrid. The method treats each inverter as an agent of a multi-agent system (i.e., the microgrid); each inverter exchanges data with a few other neighbor inverters and processes the information to update its local voltage set points and synchronize their normalized power and frequencies. The proposed controller includes three modules: voltage regulator, reactive power regulator, and active power regulator. Salient features of the proposed control methodology are as listed:

1) The voltage regulator maintains the average voltage amplitude of the microgrid at the rated value. Dynamic consensus protocol is used in the voltage regulator to estimate the average voltage across the microgrid.
2) The reactive power regulator compares local reactive loading ratio with the neighbors' and, accordingly, adjusts the voltage amplitude set point to mitigate the mismatch.
3) The active power regulator compares local active loading ratio with the neighbors' and, accordingly, adjusts the frequency set point to mitigate the mismatch. This single module handles both active power sharing and frequency synchronization.
4) Unlike existing methods, the proposed technique does not require any frequency feedback or frequency measurement, which can help to improve dynamic response of the system.
5) A sparse communication network links the sources (controllers) to exchange control variables. This network must form a connected graph. Additionally, the network shall carry some redundant links; the graph must remain connected in case of any single link failure. As long as the communication network remains connected, impairments such as delay or packet loss, may not compromise the system performance.
6) The control methodology is scalable, for that no prior knowledge of the system is required by any new source to enter and service the system.

The rest of the paper is outlined as follows: Section II reviews a preliminary of the distributed cooperative control and proposes the control methodology. Section III reviews the consensus protocol used in voltage observers. Performance of the controller is studied on a low-voltage AC microgrid, where the results are reported in Section IV. Section V concludes the paper.

II. Proposed Control Methodology

An AC distribution system, augmented with a sparse communication network, is adopted here (see Figs. 1(a) and 1(b)). For each source, attached communication links facilitate data exchange with few other sources on the other end of the link.

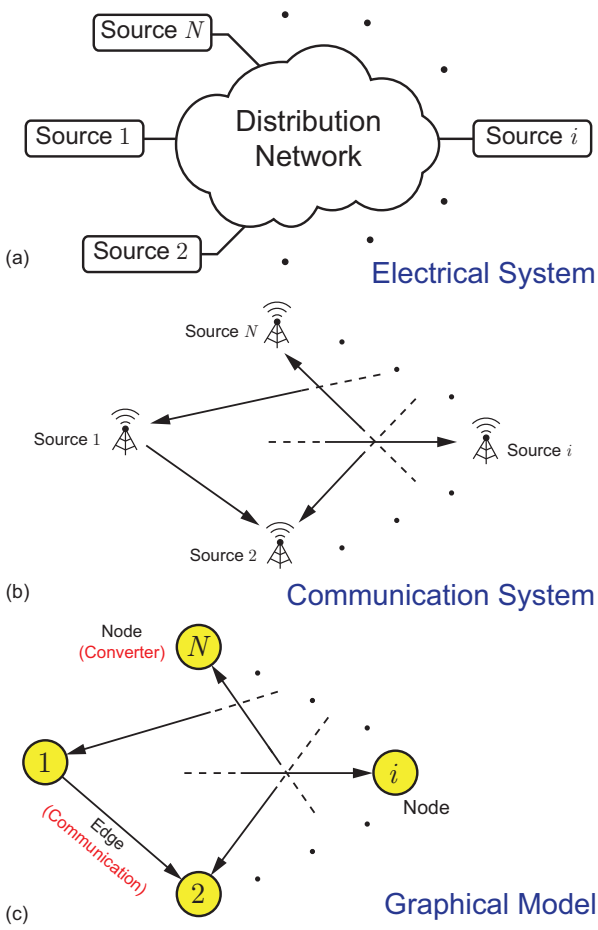

Fig. 1. General layout of an AC microgrid: (a) Sources supplying the microgrid, (b) Communication infrastructure spanned across the microgrid, (c) Graphical representation of the cyber-physical system (i.e., the microgrid).

Thus, not all sources are in contact with each other or with a centralized supervisory control. Instead, each agent exchanges control information with its neighbors; to whom the agent is directly linked on the communication graph. This cyber-physical system can be represented as a graphical interaction of dynamic agents, as shown in Fig. 1(c), where each node inherits its associated source dynamic and each edge models corresponding communication channel.

Figure 1(c) shows a typical directed communication graph (digraph) between multiple agents. Such a graph is usually represented by an associated adjacency matrix $\mathbf{A}_\mathbf{G} = \left[a_{ij}\right] \in \mathbb{R}^{N\times N}$. The Adjacency matrix $\mathbf{A}_\mathbf{G}$ carries the communication weights, where $a_{ij} > 0$ if Node i receives data from Node j and $a_{ij} = 0$ otherwise. N_i denotes the set of all neighbors of Node i. The in-degree and out-degree matrices $\mathbf{D}^{\text{in}} = \text{diag}\left\{d_i^{\text{in}}\right\}$ and $\mathbf{D}^{\text{out}} = \text{diag}\left\{d_i^{\text{out}}\right\}$ are diagonal matrices with $d_i^{\text{in}} = \sum_{j\in N_i} a_{ij}$ and $d_i^{\text{out}} = \sum_{i\in N_j} a_{ji}$, respectively. The Laplacian matrix is defined as $\mathbf{L} = \mathbf{D}^{\text{in}} - \mathbf{A}_\mathbf{G}$, whose eigenvalues determine the global dynamics of the system.

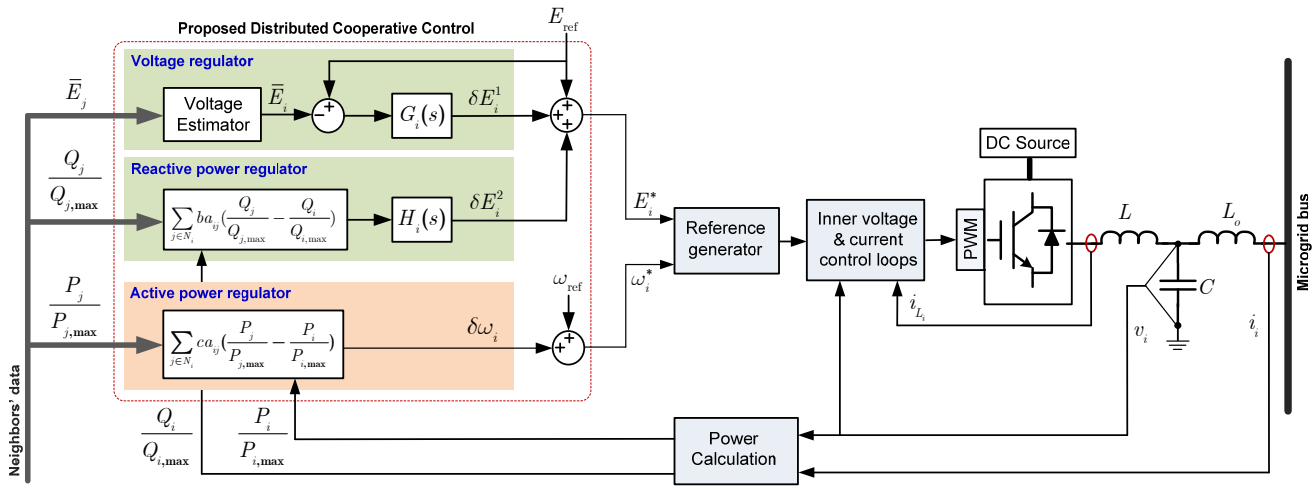

Fig. 2. Proposed secondary control for AC distribution systems; the controller at Source i.

The Laplacian matrix is balanced if the in-degree and out-degree matrices are equal, in particular, an undirected (bidirectional) data network satisfies this requirement. A direct path from Node i to Node j is a sequence of edges that connects the two nodes. A digraph is said to have a spanning tree if it contains a root node, from which, there exists at least a direct path to every other node. Here, the communication graph assumes to be *balanced*. Moreover, the graph shall carry *minimal redundancy*, i.e., in case of any link failure, the remaining links form a connected graph. Each source, e.g., Source i, exchanges an information vector $\Psi_i = \left[\bar{E}_i, Q_i/Q_{i,\max}, P_i/P_{i,\max}\right]$ to its neighbors on the communication graph, where $\bar{E}_i$, P_i, Q_i, $P_{i,\max}$, and $Q_{i,\max}$ are the estimated average voltage of the microgrid, measured active and reactive powers, and rated active and reactive powers for Source i, respectively. Herein, the second and the third elements of the information vector, Ψ_i, are called *reactive* and *active loading ratios*, respectively.

Figure 2 demonstrates schematic of the proposed cooperative control policy. Voltage regulation, frequency synchronization, and active/reactive load sharing are the main control objective in any ac system. Fine adjustment of frequency and voltage would satisfy all these objectives. Particularly, active and reactive powers respond to any change in the frequency and voltage magnitude, respectively. As highlighted in Fig. 2, the proposed controller at each source carries three modules, voltage regulator, reactive power regulator, and active power regulator.

Two voltage correction terms adjust the voltage set point for each source, i.e., $E_i^* = E_{\text{ref}} + \delta E_i^1 + \delta E_i^2$, where E_{ref} is the reference voltage (rated voltage of the system). δE_i^1 and δE_i^2 are the first and the second voltage correction terms generated by the voltage regulator and the reactive power regulator, respectively. The voltage regulator features a voltage estimator that uses dynamic consensus protocol to estimate the global average voltage across the microgrid, $\bar{E}_i$. Dynamic consensus protocol is explained the subsequent section. The estimated average voltage, $\bar{E}_i$, is then compared with the reference voltage, E_{ref}, to update the first voltage correction term, δE_i^1,

$$\delta E_i^1 = G_i(s)(E_{\text{ref}} - \bar{E}_i), \tag{1}$$

that helps to boost the voltage across the microgrid. The voltage regulator addresses the global voltage regulation defined in [25], where no individual bus voltage shall be regulated at the rated value, instead, the average of all voltages should match the rated value. The global voltage regulation allows slight voltage deviation (however, less than 5%) to provide accurate load sharing.

The reactive power regulator at ny source, e.g., Source i, compares the local reactive loading ratio, $Q_i/Q_{i,\max}$, with those of its neighbors and, accordingly, calculates the second voltage correction term, δE_i^2,

$$\delta E_i^2 = H_i(s)\left(\sum_{j\in N_i} ba_{ij}\left(\frac{Q_j}{Q_{j,\max}} - \frac{Q_i}{Q_{i,\max}}\right)\right), \tag{2}$$

where b is the coupling gain between the voltage and reactive power regulators. Upon successful operation of the voltage and reactive power regulator, the average voltage across the microgrid would satisfy the rated value and all reactive loading ratios will synchronize; which satisfies global voltage regulation and proportional reactive load sharing.

Active power regulator compares the local active loading ratio, $P_i/P_{i,\max}$, with those of its neighbors to find the active loading mismatch and, accordingly, adjusts the frequency set point as,

$$\omega_i^* = \omega_{\text{ref}} + \sum_{j\in N_i} ca_{ij}\left(\frac{P_j}{P_{j,\max}} - \frac{P_i}{P_{i,\max}}\right), \tag{3}$$

where ω_{ref} is the desired system frequency and c is a coupling gain.

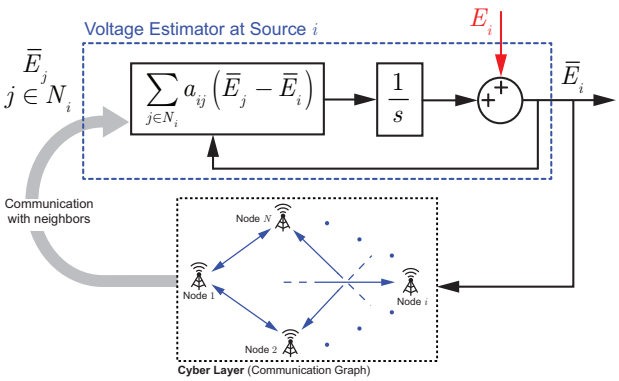

Fig. 3. Dynamic consensus protocol used at Node i to provide the average voltage of the microgrid.

In steady-state operation, the active loading ratios will converge to the same value, which provides active proportional load sharing. In addition, according to (3) all frequencies successfully synchronize to the desired value.

III. Dynamic Consensus Protocol

The estimator module at Node i (see Fig. 2) provides the average voltage amplitude across the microgrid. Figure 3 elaborates functionality of the so-called *dynamic consensus* protocol. This protocol is used as a distributed decision making approach for estimating the average voltage. According to Fig. 3, the estimator at Node i, updates its estimation based on

$$\bar{E}_i(t) = E_i(t) + \int_0^t \sum_{j\in N_i} a_{ij}\left(\bar{E}_j(\tau) - \bar{E}_i(\tau)\right)\mathrm{d}\tau, \qquad (4)$$

where E_i is the voltage amplitude of the Source i and $\bar{E}_j$ is the estimation of the average voltage amplitude provided by the estimator at Node j. As seen in (4), the updating protocol uses the local voltage, E_i, however, no other neighbors measurement is directly fed into the estimation process. Indeed, any voltage variation at any Source, e.g., at Source i, would immediately affect the estimation at that node, $\bar{E}_i$. Given a connected communication graph, the variation in $\bar{E}_i$ would propagate across the network and affect all other estimations. It is shown in [25] that if the communication graph carries a spanning tree and with a balanced Laplacian matrix, all estimations, i.e., $\bar{E}_i$s, converge to a global consensus, which is the true average of the voltage amplitudes across the microgrid. In other words,

$$\lim_{t\to\infty} \bar{E}_i(t) = \frac{1}{N}\sum_{i=1}^{N} E_i(t). \qquad (5)$$

IV. Case Study

A three-phase AC microgrid test bench, shown in Fig. 4, is adopted to study performance of the control methodology.

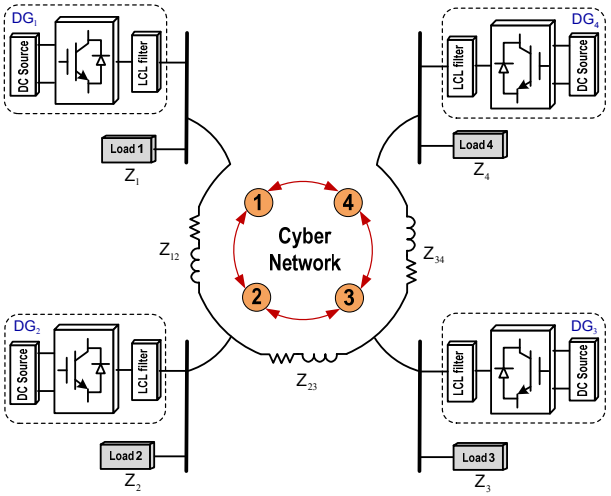

Fig. 4. Schematic of the studied AC microgrid with the highlighted communication graph.

The electric network forms a radial connection while the communication network shapes a ring. The underlying microgrid includes four Distributed Generators (DGs), with different rated powers, supplying local loads assisting remote loads. Rated powers of the DGs 1 and 2 are twice those of the DGs 3 and 4. Rated rms voltage (Line-to-Neutral) of the system is 230 V ($E_{\text{ref}} = \sqrt{2}\times 230 = 325$ V) with the frequency of 50 Hz. LCL filters are used in the outputs of the DGs to eliminate switching harmonics. Series RL impedances are used to model distribution line impedances. Detailed parameters of the microgrid are listed in Table I. The bidirectional communication network, highlighted in Fig. 4, facilitates cooperation among the DGs. It should be noted that alternative cyber structures with less links could also meet the operational requirements. However, a single spare link is considered to 1) improve the system dynamics and 2) maintain graphical connectivity in case of any single link/inverter failure.

The proposed control strategy is simulated in MATLAB Simulink®. Adjacency matrix of the cyber network, $\mathbf{A}_{\text{G}}$, and the coupling gains b and c are,

$$\mathbf{A}_{\text{G}} = \begin{bmatrix} 0 & 2.8 & 0 & 2.8 \\ 2.8 & 0 & 2.8 & 0 \\ 0 & 2.8 & 0 & 2.8 \\ 2.8 & 0 & 2.8 & 0 \end{bmatrix}, \quad b = 2, \quad c = 0.025. \qquad (6)$$

Performance of the cooperative controller is evaluated through subsequent studies:

A. Transient Response to Load Change

All sources of the microgrid are initially commanded with identical voltage set points; $E_i^* = 325$ V and $\omega_i^* = 2\pi\times 50$ rad/s. The inner control loops of the driving inverters produce the gating signals according to the desired voltage amplitudes and frequencies.

TABLE I
MICROGRID TEST BENCH ELECTRICAL AND CONTROL PARAMETERS

	Parameters		Value	
	Symbol	Quantity		
Electrical Test System	V_{dc}	DC voltage	650 V	
	E^{ref}	MG voltage amplitude	325 V	
	f	MG frequency	50 Hz	
	C	LCL filter capacitance	25 µF	
	L	LCL filter inductance	1.8 mH	
	L_o	LCL filter impedance	1.8 mH	
	Z_1 , Z_2	Load 1, Load 2	$300+j314\ \Omega$	
	Z_3 , Z_4	Load 3, Load 4	$150+j157\ \Omega$	
	Z_{12}	Line impedance 1, 2	$R_{12}=1.2\ \Omega,\ L_{12}=5.4$ mH	
	Z_{23}	Line impedance 2, 3	$R_{23}=0.4\ \Omega,\ L_{23}=1.8$ mH	
	Z_{34}	Line impedance 3, 4	$R_{34}=0.4\ \Omega,\ L_{34}=3.2$ mH	
Control Parameters	Symbol	Quantity	DGs 1 & 2	DGs 3 & 4
	P_{max}	Rated active power	2200 W	1100 W
	Q_{max}	Rated active power	2200 VAr	1100 VAr
	k_{pQ}	Q sharing P term	0.01	0.01
	k_{iQ}	Q sharing I term	7	7
	k_{pv}	Voltage control P term	0.008	0.008
	k_{iv}	Voltage control I term	4	4

Figures 5 and 6 show the voltage regulation and load sharing performance for $t < 15$ s, where the proposed controller is still inactive. It can be seen that all the voltages are less than the desired value due to the voltage drop across the LCL filters. In addition, the load sharing is compromised. Indeed, sources with less rating deliver more power.

The proposed controller is then activated at $t = 15$ s. The outer voltage feedback loops are activated to compensate for the voltage drop of the LCL filters. In addition, the voltage and reactive power regulators cooperate to generate voltage correction terms, $\delta E_i = \delta E_i^1 + \delta E_i^2$, (see Fig. 5(c)) to ensure global voltage regulation and proportional reactive load sharing. As seen in Fig. 5(a), the average voltage across the microgrid is successfully regulated on the desired value of 325 V, i.e., $(1/N)\sum_{i=1}^{N} E_{Bi} = E_{ref}$. It is noteworthy that although the bus voltages are different than the rated voltage, voltage deviations are kept within an acceptable range. This voltage difference is essential to manage the reactive power flow. Reactive load sharing performance is studied in Fig. 5(b) where the reactive power is shown to be perfectly shared among DGs in proportion to their ratings.

Frequency and supplied active powers of the DGs are presented in Fig. 6. Prior to the controller activation, i.e., for $t < 15$ s, the DG frequencies are all synchronized, however, poor active power sharing is reported. Similar to Fig. 5(b), the DGs with less power rating provide the majority of the load demand. By controller activation at $t = 15$ s, the power regulators have collectively varied the frequencies to gain the desired active power sharing. It should be noted that the power regulator do not deviate the frequency set points in the steady state; however, transient variation of the frequencies tunes the phase angles to navigate the active powers and provide proportional load sharing.

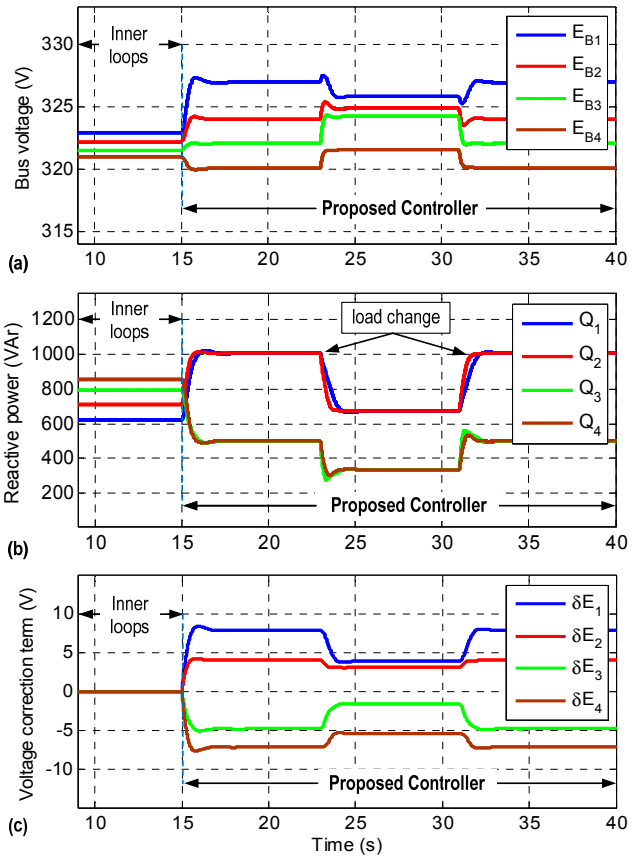

Fig. 5. Performance of the proposed controller in case of a load change: (a) Voltage regulation, (b) Proportional reactive power sharing, (c) Voltage correction terms.

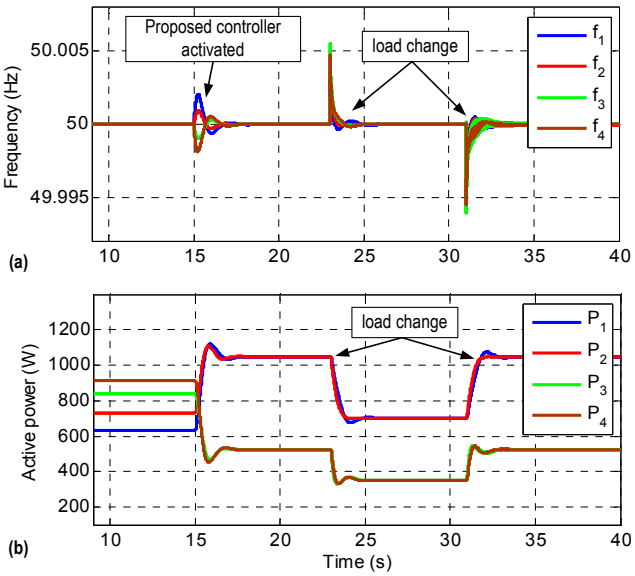

Fig. 6. Performance of the proposed controller in case of a load change: (a) Frequency synchronization, (b) Proportional active power sharing.

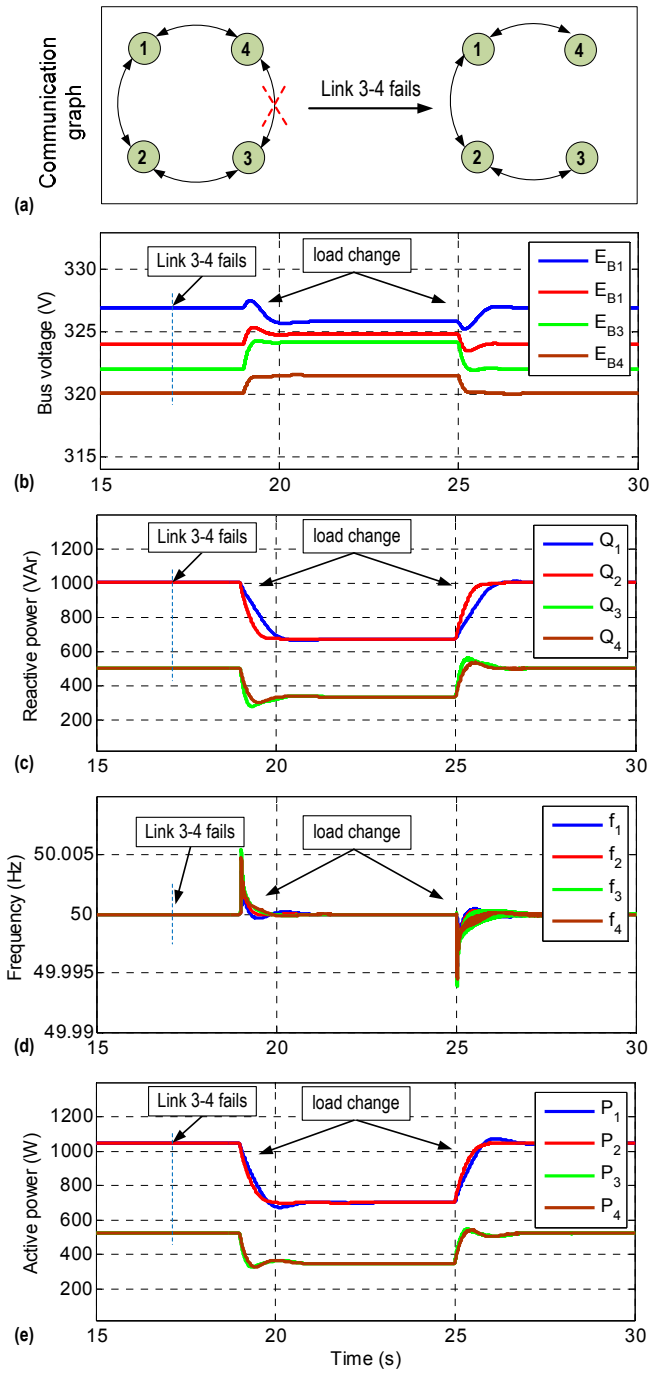

Fig. 7. Resiliency to communication link failure: (a) Communication graph, (b) Bus voltages, (c) Supplied reactive powers (d) Frequencies, (e) Supplied active powers.

Controller response to step load change is studied next. The local load at Bus 3 is unplugged at $t = 23$ s and plugged back in at $t = 32$ s. As seen in Figs. 5 and 6, global voltage regulation, frequency synchronization and proportional load sharing are perfectly carried out during the load transients. Figures 5(c) and 6(a) show how the voltage, reactive power, and active power regulators respond to load change and readjust the voltage set points and phase angles to maintain voltage regulation and proportional load sharing.

B. Communication-Link Failure Resiliency

Efficacy of the controller is practiced during a step load change with a failed link. The communication Link 3-4 (between DGs 3 and 4) is intentionally disabled at $t = 17$ s. As seen in Fig. 7, the link failure does not impact voltage regulation or load sharing in the microgrid, for that the link failure does not compromise connectivity of the communication graph. Figure 7(a) demonstrates how the graph reconfigures in respond to Link 3-4 failure. It can be seen in Fig. 7(a) that the new graph is still connected, thus, the controller shall remain operative. However, any loss of connection affects the Laplacian matrix and, thus, the system dynamic. Generally, less communication links limits the information flow and slows down the transient response of the system. Load changes are then introduced with the failed link at moments $t = 19$ s and $t = 25$ s. It can be observed from Fig. 7 that the voltage regulation and active/reactive load sharing are successfully handled. However, comparing Figs. 5(b) and 7(c) implies that the system dynamic has slowed down in Fig. 7(c) due to the loss of a communication link. Similarly, Fig. 6(b) shows a faster response in comparison to Fig. 7(e).

C. Loss of a Source

Controller response to a DG failure is an important study since it is a common contingency in microgrids. Accordingly, the inverter driving DG 3 is intentionally turned off at $t = 17$ s to practice loss of the Source 3. Practically, loss of a source follows by the loss of all communication links attached to that particular source. Figure 8(a) illustrates how the communication network reconfigures after the loss of Source 3. It can be seen that the network remains connected and, thus, the controller is expected to remain operational. Figure 8 shows the voltage, frequency, and the supplied powers for all DGs before and after the loss of DG 3. After the loss of this source, the global voltage regulation and frequency synchronization are preserved and the excessive load is proportionally shared among the remaining sources. It may be observed that the active/reactive powers supplied to Bus 3 do not promptly drop to zero. This is due to the low-bandwidth filters applied to the power measurements to smoothen the readings and eliminated undesired noises.

V. Conclusion

A cooperative control framework is introduced that handles voltage regulation, frequency synchronization and proportional load sharing in AC microgrids. The microgrid is augmented with a cyber network for data exchange. Each controller broadcasts an information vector to neighbor controllers, to whom it is directly linked in the cyber domain.

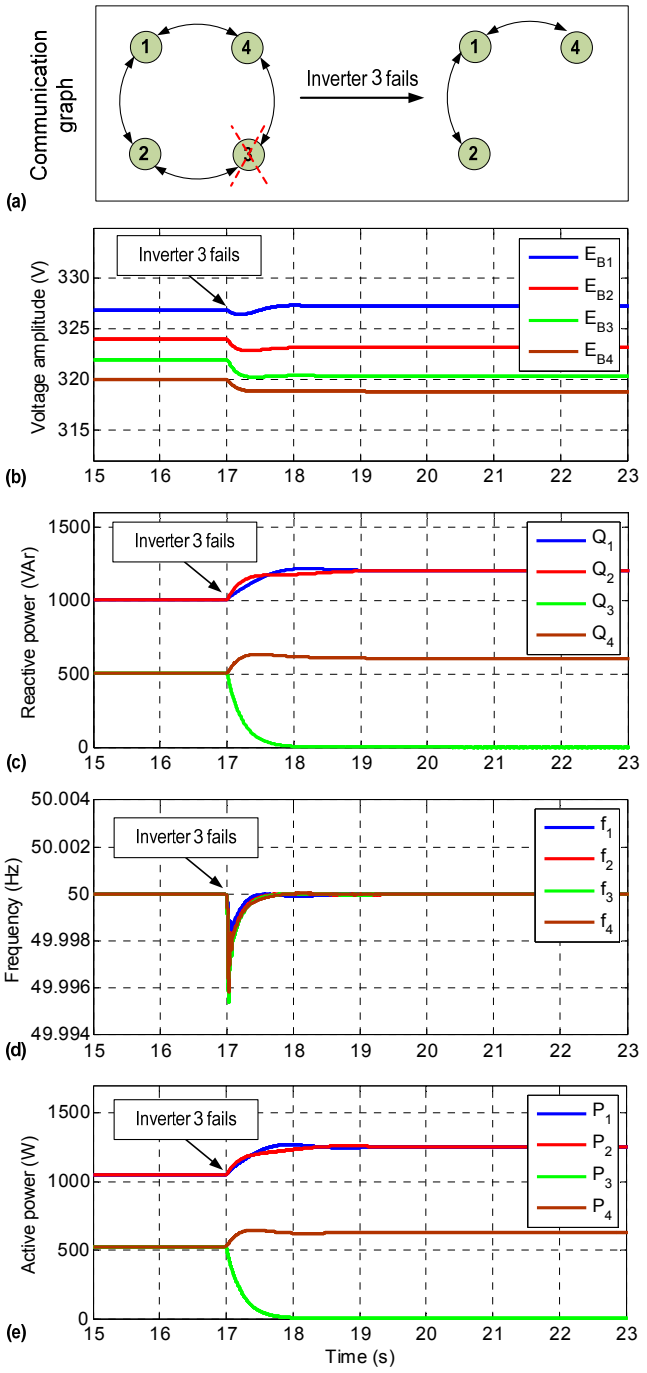

Fig. 8. Failure of a source: (a) Communication graph, (b) Bus voltages, (c) Supplied reactive powers (d) Frequencies, (e) Supplied active powers.

Each controller processes local and neighbors' information through three separate modules; the voltage regulator, the reactive power regulator, and the active power regulator. The voltage regulator uses dynamic consensus protocol to estimate the average voltage across the microgrid, which is further used to implement global voltage regulation. The reactive power regulator dynamically adjusts the local voltage set point through comparison of the local and neighbors' supplied reactive powers. Similarly, the active power regulator adjusts the local frequency set point through comparison of the local and neighbors' supplied active powers. Simulation studies show that the proposed controller successfully carries out the global voltage regulation, frequency synchronization, and proportional load power sharing.

REFERENCES

[1] R. Majumder, B. Chaudhuri, A. Ghosh, R. Majumder, G. Ledwich, and F. Zare, "Improvement of stability and load sharing in an autonomous microgrid using supplementary droop control loop," *IEEE Trans. Power Syst.*, vol. 25, no. 2, pp. 796–808, May 2010.

[2] M. Datta, T. Senjyu, A. Yona, T. Funabashi, and C. H. Kim, "A frequency-control approach by photovoltaic generator in a PV-diesel hybrid power system," *IEEE Trans. Energy Convers.*, vol. 26, no. 2, pp. 559–571, Jun. 2011.

[3] C. K. Sao and W. Lehn, "Control and power management of converter-fed microgrids," *IEEE Trans. Power Syst.,* vol. 23, pp. 1088–1098, Aug. 2008.

[4] J. C. Vasquez, J. M. Guerrero, J. Miret, M. Castilla, and L.G. de Vicuña, "Hierarchical control of intelligent microgrids," *IEEE Ind. Electron. Mag.*, vol. 4, pp. 23–29, Dec. 2010.

[5] A. Bidram and A. Davoudi, "Hierarchical structure of microgrids control system," *IEEE Trans. Smart Grid*, vol. 3, pp. 1963–1976, Dec 2012.

[6] J. A. P. Lopes, C. L. Moreira, and A. G. Madureira, "Defining control strategies for microgrids islanded operation," *IEEE Trans. Power Syst.,* vol. 21, pp. 916–924, May 2006.

[7] F. Katiraei, M. R. Iravani, and P. W. Lehn, "Microgrid autonomous operation during and subsequent to islanding process," *IEEE Trans. Power Del.,* vol. 20, pp. 248–257, Jan. 2005.

[8] C. Chen, S. Duan, T. Cai, B. Liu, and G. Hu, "Optimal allocation and economic analysis of energy storage system in microgrids," *IEEE Trans. Power Electron*., vol. 26, no. 10, pp. 2762–2773, Oct. 2011.

[9] T. L. Vandon, B. Meersman, J. D. M. De Koonig, and L. Vandevelde, "Analogy between conventional grid control and islanded microgrid control based on a global DC-link voltage droop," *IEEE Trans. Power Del.*, vol. 27, pp. 1405–1414, July 2012.

[10] A. H. Etemadi, E. J. Davison, R. Iravani, "A decentralized robust strategy for multi-DER microgrids – Part I: Fundamental concepts," *IEEE Trans. Power Del.*, vol. 27, pp. 1843–1853, Oct. 2012.

[11] A. Micallef, M. Apap, C. Spiteri-Staines, J. M. Guerrero, and J. C. Vasquez, "Reactive power sharing and voltage harmonic distortion compensation of droop controlled single phase islanded microgrids," *IEEE Trans. Smart Grid*, vol. 5, pp. 1149–1158, May 2014.

[12] A. Mehrizi-Sani and R. Iravani, "Potential-function based control of a microgrid in islanded and grid-connected modes," *IEEE Trans. Power Syst.,* vol. 25, pp. 1883–1891, Nov. 2010.

[13] A. Kahrobaeian and Y. A. R. I. Mohamed, "Networked-based hybrid distributed power sharing and control of islanded micro-grid systems," *IEEE Trans. Power Electron.*, vol. 30, no. 2, pp. 603–617, Feb. 2015.

[14] Q. Hui and W. Haddad, "Distributed nonlinear control algorithms for network consensus," *Automatica*, vol. 42, pp. 2375–2381, Sept. 2008.

[15] J. Fax and R. Murray, "Information flow and cooperative control of vehicle formations," *IEEE Trans. Automat. Control*, vol. 49, pp. 1465–1476, Sept. 2004.

[16] Z. Qu, *Cooperative control of dynamical systems: Applications to autonomous vehicles*. New York: Springer-Verlag, 2009.

[17] Q. Shafiee, C. Stefanovic, T. Dragicevic, P. Popovski, J. C. Vasquez, and J. M. Guerrero, "Robust networked control scheme for distributed secondary control of islanded microgrids," *IEEE Trans. Ind. Electron.*, vol. 61, pp. 5363–5374, Oct. 2014.

[18] Y. Zhang and H. Ma, "Theoretical and experimental investigation of networked control for parallel operation of inverters," *IEEE Trans. Ind. Electron.*, vol. 59, pp. 1961–1970, Apr. 2012.

[19] M. N. Marwali and A. Keyhani, "Control of distributed generation systems – Part I: Voltages and currents control," *IEEE Trans. Power Electron.*, vol. 19, pp. 1541–1550, Nov. 2004.
[20] M. N. Marwali, J. W. Jung, and A. Keyhani, "Stability analysis of load sharing control for distributed generation systems," *IEEE Trans. Energy Convers.*, vol. 22, pp. 737–745, Sept. 2004.
[21] S. D. J. McArthur, E. M. Davidson, V. M. Catterson, A. L. Dimeas, N. D. Hatziargyriou, F. Ponci, and T. Funabashi, "Multi-agent systems for power engineering applications – part I: Concepts, approaches, and technical challenges," *IEEE Trans. Power Syst.,* vol. 22, pp. 1743–1752, Nov. 2007.
[22] A. Bidram, A. Davoudi, and F. L. Lewis, "A multi-objective distributed control framework for islanded microgrids," *IEEE Trans. Ind. Informatics*, vol. 10, no. 3, pp. 1785–1798, Aug. 2014.
[23] V. Nasirian, A. Davoudi, and F. L. Lewis, "Distributed adaptive droop control for DC microgrids," in *Proc. 29th IEEE Appl. Power Electron. Conf. Expo. (APEC)*, 2014, pp. 1147–1152.
[24] Q. Shafiee, V. Nasirian, J. M. Guerrero, F. L. Lewis, and A. Davoudi, "Team-oriented adaptive droop control for autonomous AC microgrids," in *Proc. 40th IEEE Annu. Conf. Ind. Electron. Soc. (IECON)*, 2014, pp. 1861–1867.
[25] V. Nasirian, S. Moayedi, A. Davoudi, and F. L. Lewis, "Distributed cooperative control of DC microgrids," *IEEE Trans. Power Electron.*, vol. 30, no. 4, pp. 2288–2303, Apr. 2015.
[26] V. Nasirian, A. Davoudi, F. L. Lewis, and J. M. Guerrero, "Distributed adaptive droop control for DC distribution systems," *IEEE Trans. Energy Convers.*, to be published, DOI: 10.1109/TEC.2014.2350458.
[27] S. Moayedi, V. Nasirian, F. L. Lewis, and A. Davoudi, "Team-oriented load sharing in parallel DC-DC converters," *IEEE Trans. Ind. Appl.*, to be published, DOI: 10.1109/TIA.2014.2336982.
[28] B. A. Robbins, C. N. Hadjicostis, and A. D. Dominguez-Garcia, "A two-stage distributed architecture for voltage control in power distribution systems," *IEEE Trans. Power Syst.*, vol. 28, pp. 1470–1482, May 2013.
[29] J. W. Simpson-Porco, F. Dorfler, and F. Bullo, "Synchronization and power sharing for droop-controlled inverters in islanded microgrids," *Automatica*, vol. 49, pp. 2603–2611, Jun. 2013.